

Letters

Dispersed Structure and Rheology of Lipophilized-Smectite/Toluene Suspensions

Masami Okamoto,^{*,†} Hideyuki Taguchi,[†] Harumi Sato,[†] Tadao Kotaka,[†] and
Hiroshi Tateyama[‡]

*Advanced Polymeric Materials Engineering, Graduate School of Engineering,
Toyota Technological Institute, Hisakata 2-12-1, Tempaku, Nagoya 468-8511, Japan,
and Inorganic Materials Department, Kyushu National Industrial Research Institute,
Shuku-machi, Tosu-shi 841-0052, Japan*

Received July 13, 1999. In Final Form: March 6, 2000

Dispersed rheology of lipophilized-smectite (SAN)/toluene (TOL) suspensions with various concentrations ϕ of $(0.03-3.77) \times 10^{-2}$ vol fraction was examined by a stress-controlled rheometer and Ubbelohde type viscometer. Under the quiescent state of the SAN/TOL suspensions, the original laminate structure in the solid state of SAN was lost and exfoliation of the silicate layers took place as revealed by X-ray diffraction analysis. In the dilute SAN/TOL suspension with $10^2\phi \leq 0.2$, the value of η_{sp}/ϕ (η_{sp} being specific viscosity) is independent of concentration up to $\phi \sim 2 \times 10^{-3}$ and exhibits abrupt increasing beyond $\phi \sim 2 \times 10^{-3}$. The dense concentration region exhibits elastic gel-like properties, and rheopexy behavior imposed by shear stress was observed. The limiting value of the dynamic storage modulus G' was given by $G'(\omega \rightarrow 0) \sim \phi^4$, whereas the loss tangent δ exhibited independence of ϕ and remains at a constant value of about 0.1.

Introduction

Generally, aqueous suspensions of clay are more or less flocculated and exhibit remarkable long-term gelation and yield stress thixotropic and rheopexy behavior as reported by van Olphen¹ some 20 years ago. In dilute suspensions of smectite swelling clays such as hectorite and montmorillonite, there are two aspects of the gelation mechanism: One is a formation of a microfloculation due to electrostatic attraction between the positively charged edges and negatively charged faces of the platelike particles, resulting in a card-house structure. Another, suggested by Norrish,² is the effect of long-range elec-

trostatic repulsion between interaction double layers, which leads to an equilibrium structure. However, it is difficult to select between attractive and repulsive interparticle interactions during gelation of suspensions.

Very recently, the existence of a long-range structural correlation (~ 100 nm) was proposed via an in situ neutron scattering experiment of the smectite suspension under quiescent state.³ This will be one noteworthy hypothesis for new interpretation of gelation and complex rheological properties.

In our previous paper,⁴ we synthesized clay/polymer nanocomposites with organically modified smectic clay and investigated the rheology of both suspensions (before polymerization) and clay/polystyrene nanocomposites. In

* To whom correspondence may be addressed. Fax: +81-52-809-1864. E-mail: okamoto@toyota-ti.ac.jp.

[†] Toyota Technological Institute.

[‡] Kyushu National Industrial Research Institute.

(1) van Olphen, H. *An Introduction to Clay Colloid Chemistry*; Wiley: New York, 1977.

(2) Norrish, K. *Discuss. Faraday Soc.* **1954**, *18*, 120.

(3) Mourchid, A.; Delville, A.; Lambard, J.; Lecolier, E.; Levitz, P. *Langmuir* **1995**, *11*, 1942.

(4) Sato, H.; Taguchi, H.; Sato, N.; Okamoto, M.; Kotaka, T. In *Proc. SPSJ Annu. Meeting, 46th* **1997**, E, 144-145. Okamoto, M.; Morita, S.; Taguchi, H.; Kim, Y. H.; Kotaka, T.; Tateyama *Polymer* **2000**, *41*, 3887.

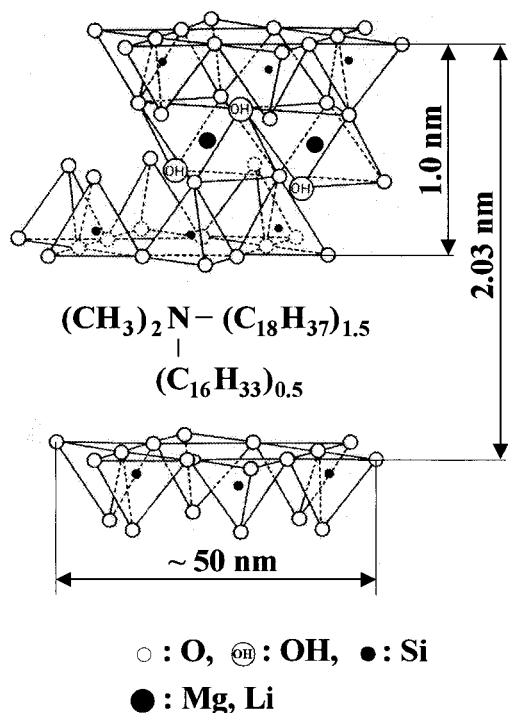


Figure 1. Crystal structure of SAN powder.

the lipophilized smectite/styrene gel-like suspensions, the thixotropic recovery and rheopexy under shear flow were observed to resemble the aqueous suspensions of the clay. A better understanding of the rheological and structural analyses of the suspensions and subsequent preparation of the nanocomposites are of fundamental importance in controlling the nanoscale structure.

In this paper, we aim to confirm the measurement of dynamic properties under oscillatory shear, and flow behavior under stress-sweep shear conditions, which are related to the internal structure of the suspensions in practically, are discussed.

Experimental Section

Synthetic smectite consists of an octahedral $\text{AlO}_4(\text{OH})_2$ sheet sandwiched between two SiO_4 tetrahedral layers (~1 nm thick and ~50 nm in diameter) with the charges being adjusted by substituting Al^{3+} or Si^{4+} with Mg^{2+} and/or Li^+ and the depressed charges being neutralized with alkaline cations intercalated into the interlayer spaces to form a laminate structure of several hundred layers. The clay sample studied was lipophilized-smectite clay (CO-OP Chemical) obtained from hydrophilic smectite, intercalated with Na^+ ions, $\text{Na}_{0.33}(\text{Mg}_{2.67}\text{Li}_{0.33})\text{Si}_4\text{O}_{10}(\text{OH})_2$ (cation exchange capacity of 86.6 mequiv/100 g), by substituting them with quarternized ammonium salt (QA) such as hexadecyltadecylammonium chloride, $[(\text{C}_{16}\text{H}_{33})_{0.5}(\text{C}_{18}\text{H}_{37})_{1.5}\text{N}^+(\text{CH}_3)_2]\text{Cl}^-$ (SAN), as shown in Figure 1.

We can evaluate that about 100 QA molecules are localized near the individual clay layers ($\sim 8 \times 10^{-15} \text{ m}^2$) by technical data from the supplier.⁵

Instead of using styrene monomer, we used commercial grade toluene (TOL) (EP-grade, Tokyo-Kasei Co.) because it had no polymerization effect on the measurement.

SAN/TOL suspensions with various concentrations of 0.1–20 wt % (volume fraction $10^2\phi = 0.03$ –3.77) were prepared via ultrasonication (Ultrasonic 250, Hey Co.) at 50–60 °C usually for 60 min to obtain a transparent suspension. Sonicated suspensions were allowed to stand still in sealed grass tubes for 24 h at room temperature and then were subjected to the measurements. In our suspensions, the calculated ionic strength was a very low value of $\sim 10^{-4} \text{ mol dm}^{-3}$.⁴

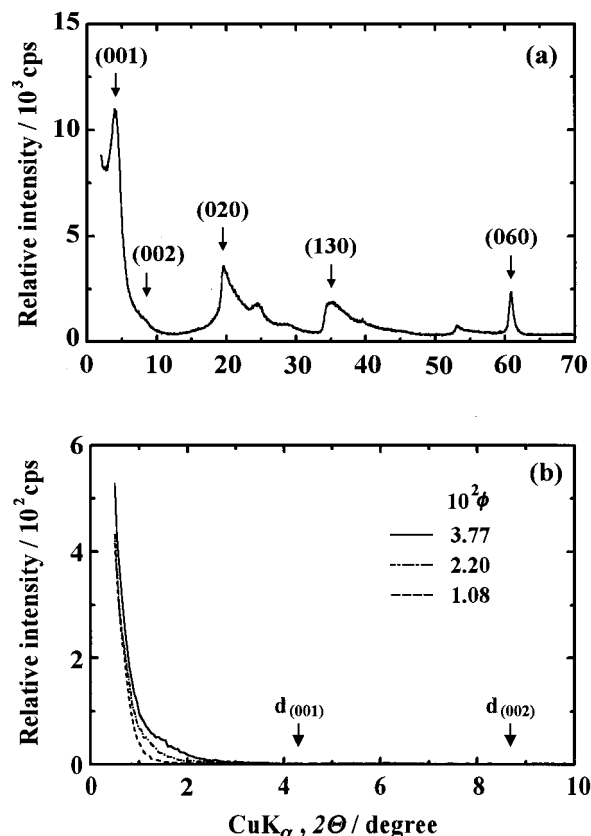


Figure 2. X-ray diffractograms of (a) SAN powder and (b) SAN/TOL suspensions with three different concentrations. The arrows in panel b indicate the (001) and (002) reflections of SAN.

X-ray diffraction (XRD) experiments were performed directly for the SAN solid and SAN/TOL suspensions with various compositions by a Philips PW3050 diffractometer with graphite monochromator using $\text{Cu K}\alpha$ radiation at 40 kV and 50 mA. For the dilute suspensions ($10^2\phi \leq 1.0$), viscosity measurements were performed by a Ubbelohde type viscometer at 25 °C. Dynamic viscoelastic and stress-sweep measurements for dense concentrations ($10^2\phi > 1.0$) were carried out on a Rheometrics stress rheometer (DSR200) with a cone–plate geometry of cone angle 0.04 rad and diameter 40.0 mm operated under a solvent-sealed chamber at 25 °C.

Results

Figure 2a shows the X-ray diffractogram of SAN powder. An interlayer spacing $d_{(001)}$ of the (001) plane larger than that of Na^+ -type smectite (2.03 nm compared to 1.20 nm) was found,⁴ suggesting the QA molecules are intercalated in the silicate layers as shown in Figure 1. The (002) reflection of SAN, however, is not clearly a peak but is a very small shoulder around the diffraction angle $2\theta = 8.0^\circ$. The well-ordered lamellar structure as seen in Na^+ -type smectite cannot be seen in this SAN powder. For the suspensions with three different concentrations ($10^2\phi = 1.08$ –3.77), clearly the peaks of the (001) and (002) reflections of SAN (indicated by arrows in the figure) disappeared as seen in Figure 2b. The delamination and dispersion of the silicate layers are retained in each concentration. For the suspensions with $10^2\phi < 1.08$, unfortunately we cannot obtain a sufficient intensity for analysis of the diffractogram.

The complete exfoliation of the silicate layers, however, cannot clearly be determined by using XRD analysis. We should use light scattering (LS) measurements to confirm the existence of a large-scale flocculated structure in the suspensions.

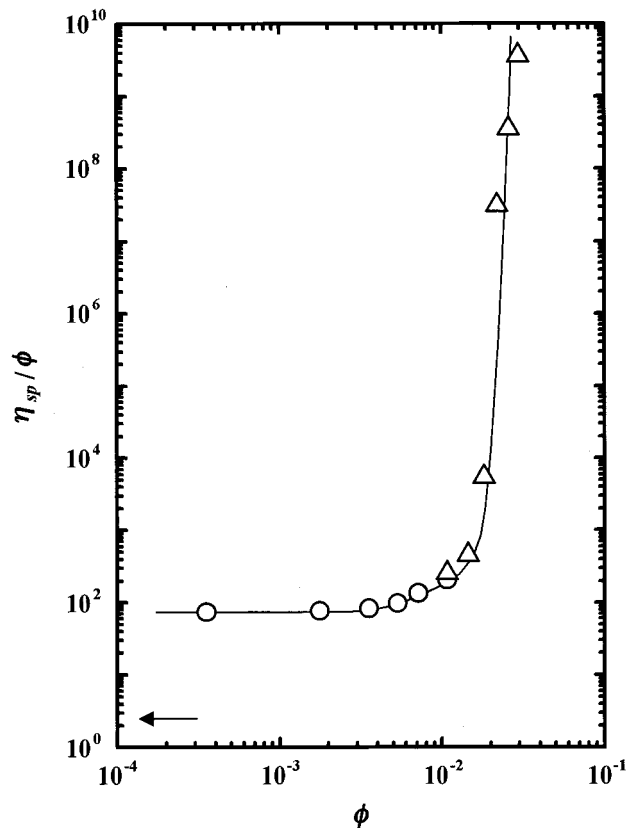


Figure 3. Double logarithmic plot of η_{sp}/ϕ vs ϕ . The circles are the data for dilute concentration and triangles are data for the dense condition obtained by the stress-sweep test.

We attempted to determine the viscosity at dilute suspensions by using a Ubbelohde type viscometer. Figure 3 shows a double logarithmic plot of specific viscosity η_{sp} ($=[\eta_{SAN/TOL}/\eta_{TOL}] - 1$) vs ϕ curve in the concentration range of 0.03×10^{-2} to 0.01. Here, the vertical axis is reduced by ϕ because of discussion in accordance with the modified Einstein equation derived by Batchelor.⁶ The value of η_{sp}/ϕ is independent of concentration up to $\phi \sim 2 \times 10^{-3}$ and exhibits abrupt increasing beyond $\phi \sim 2 \times 10^{-3}$. The data indicated by triangles in Figure 3 are for the dense suspensions obtained by the stress-sweep shear test as described later. Here we calculated the shear stress under capillary flow in a Ubbelohde viscometer by using the Haagen–Poiseuille equation, and the value of viscosity η corresponding to the calculated shear stress was collected.

All data points nicely fall into a single curve, suggesting the big difference of viscosity is due to the internal structural change in the suspensions between dilute and dense concentration regions.

For dense conditions ($10^2\phi > 1.0$), the SAN/TOL suspensions exhibit elastic gel-like properties after ultrasonic preparation. Figure 4 shows the typical frequency ω dependence linear viscoelasticity. We can clearly see that both moduli are almost independent of ϕ and the value of $G'(\omega)$ is larger than $G''(\omega)$ within a frame work of ω , suggesting the system is a viscoelastic solidlike gel. Furthermore, the increment of both moduli with increasing ϕ evolves by an order of magnitude.

At the end of a long relaxation time ($\omega \sim 0.1$ rad/s), the plateau $G'(\omega)$ exhibits increasing viscosity ($\cong G'(\omega)/\omega$). This tendency resembles the relaxation of the internal developed structure or rheopecty behavior as described later.

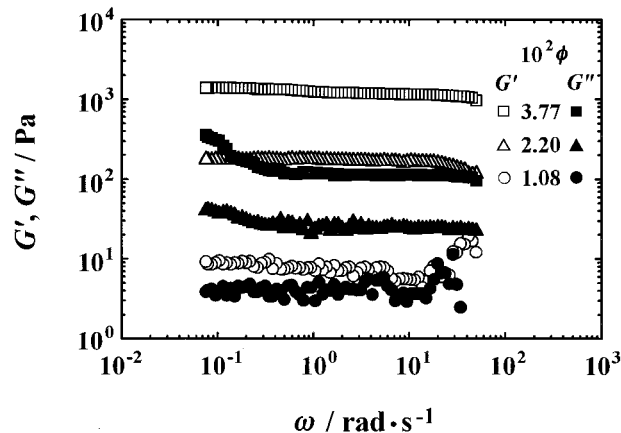


Figure 4. Frequency ω response of the storage $G'(\omega)$ and loss $G''(\omega)$ moduli of SAN/TOL suspensions with three different concentrations.

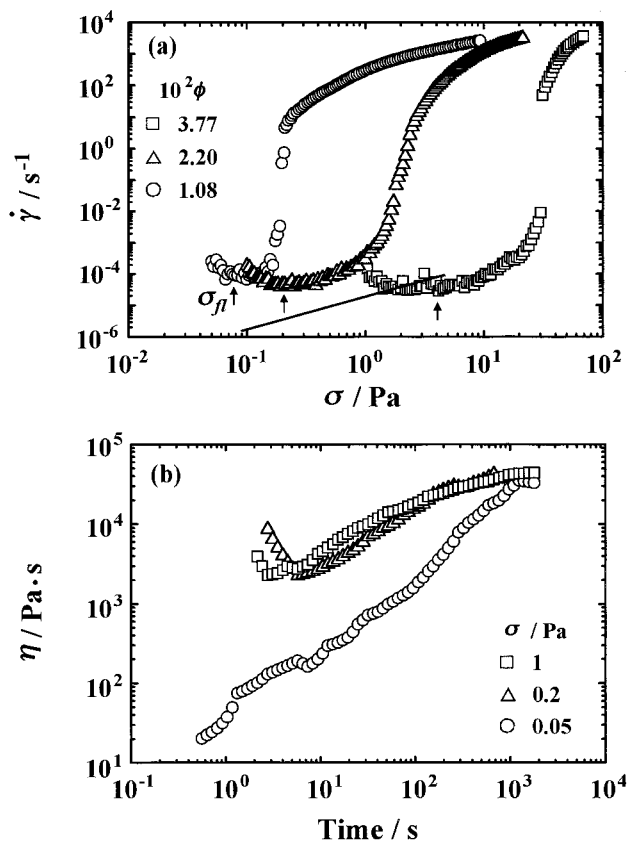


Figure 5. (a) Typical flow curves for dense SAN/TOL suspensions of various concentrations under a stress-sweep test. (b) Time evolution of shear viscosity η under the constant shear stress σ . In panel (a) the arrows indicate the apparent fluidizing points σ_f . Under zero sweep rate the shear rate $\dot{\gamma}$ vs shear stress σ curve becomes the solid line as shown in (a).

Figure 5 shows typical flow curves of the dense suspensions of the SAN/TOL system under the stress-sweep run in which shear rate $\dot{\gamma}$ is plotted against imposed shear stress σ . Note here, each suspension with different ϕ values begins to flow at a certain point, but the $\dot{\gamma}$ decreases with increasing σ for a short while, and then at another point σ_f (apparent fluidizing point, indicated by arrows in Figure 5) the $\dot{\gamma}$ increases suddenly by a factor of 10^5 – 10^6 while σ is the only doubled increment (pseudo-plastic or shear thinning regime). The question here is, does such thixotropic behavior strongly depend on the sweep rate or not? To clarify this point, we examined time

(6) Batchelor, G. K. *J. Fluid Mech.* **1977**, *83*, 97.

dependence of η (and/or $\dot{\gamma}$) under constant σ mode. Figure 5b shows the typical example of the time evolution of η under three different constants (σ) of SAN/TOL suspension with $10^2\phi = 2.2$.

In the early stage (<10 s), η slightly decreases as in the case of $\sigma > 0.2$ Pa, attains a minimum (~ 6 s), and then increases with time and finally levels off at 2000 s in each σ . Note here, the final values of η reach the same steady state value; i.e., the system becomes a Newtonian fluid. The inserted solid line for $10^2\phi = 2.2$ in Figure 5a is the final steady-state relation between $\dot{\gamma}$ and σ at various σ conditions. That is, this thixotropic behavior obtained from the stress-sweep test is presumably in a quasi-equilibrium state. This may imply that the long time relaxation of the system is taking place with the structural change. In other words, the flow-induced internal structure development, e.g., deflocculation and/or flocculation of dispersed structure of smectite in TOL, may proceed with a long time scale ($>10^3$ s).

Discussion

We attempt here to estimate the existence of a large thin disklike flocculated structure with large anisotropy according to Simha's treatment in dilute aqueous suspensions developed some 60 years ago.⁷

For the case of aspect ratio $f \gg 1$ of disklike particles with non-Newtonian flow of the dispersed particles on the assumption of $\dot{\gamma}/D_{\text{rot}} \rightarrow 0$ (D_{rot} being the rotational diffusion constant of the particles $\sim 10^4$ – 10^5 s⁻¹), η_{sp}/ϕ is given by

$$\left[\frac{\eta_{\text{sp}}}{\phi} \right]_{\dot{\gamma}/D_{\text{rot}} \rightarrow 0} \cong \frac{16f}{15 \tan^{-1} f} \quad (1)$$

In our SAN/TOL dilute suspensions, this assumption may be acceptable because $\dot{\gamma}$ is about 10^2 – 10^3 s⁻¹ in our test condition of the viscometer. From the result in Figure 3, we obtained f of about 120 employing eq 1. We can

speculate the large disklike structure, compared to the monolayer structure of SAN ($f \sim 50$), may disperse randomly without any interaction between another disks in the TOL medium in the dilute SAN/TOL suspensions with $10^2\phi \leq 1.0$.

On the other hand, in the gelation region, the abrupt increasing of viscosity with a very small increment of ϕ in the dense condition ($10^2\phi > 1.0$) may be the sol/gel transition with formation of a spatial spherical structure, i.e., proceeding of both the flocculation and aggregation. The origin of the rheoexy behavior up to σ_{fl} is presumably the relaxation of the spatial-linked structure by imposing the stress because of the suppression of self-diffusion.

In this region, the power law relation for both zero- ω limiting value of modulus $G'(\omega \rightarrow 0)$ and σ_{fl} were obtained as follows:

$$G'(\omega \rightarrow 0) \sim \sigma_{\text{fl}} \propto \phi^\alpha \quad (2)$$

The obtained exponent α of about 4.0 is a higher value than that of about 3 reported by Ramsay.⁸ Presumably this system is strongly flocculated compared to Ramsay's aqueous suspension system. Interestingly, the ratio of $G'(\omega)/G'(\omega)$ ($=\tan \delta$) exhibits independence of ϕ and remains constant at a value of about 0.1. This behavior presumably relates to self-similarity of the linked structure in the gelation region reported by Winter.⁹

Finally, by imposing the constant stress, the deflocculation and/or flocculation of the structure may occur as revealed by increasing of η with time (cf. Figure 5b). To understand this behavior, we should try to look into the internal structure under shear flow. We must also construct the rheo-optical device, small-angle LS apparatus under shear flow. This is currently under way in our laboratory and will be clarified shortly.¹⁰

LA990933C

(8) Ramsay, J. D. F. *J. Colloid Interface Sci.* **1986**, *109*, 441.

(9) Winter, H. H.; Chambon, F. *J. Rheol.* **1986**, *30*, 367.

(10) Okamoto, M.; Sato, H.; Taguchi, H.; Kotaka, T. To be submitted for publication in *Langmuir*.

(7) Simha, R. *J. Phys. Chem.* **1940**, *44*, 25.